Properties of $(GaAs)_{1-x}Ge_{2x}$ and $(GaSb)_{1-x}Ge_{2x}$: Consequences of a stochastic growth process

L. C. Davis and H. Holloway
Ford Motor Company, Research Staff, P.O. Box 2053, Dearborn, Michigan 48121-2053
(Received 11 September 1986)

A new model is presented for the structure of the pseudobinary alloys of the III-V semiconductors GaAs and GaSb with the group IV semiconductor germanium. This model is based upon the random arrival of the constituent atoms at the growing {100} surface. The main postulates are that Ga—Ga and As—As or Sb—Sb nearest-neighbor pairs are prohibited and that each incorporated Ga atom acquires a nearest-neighbor As (or Sb) atom from the excess of the group V constituent that is present during growth. The model has been implemented by Monte Carlo simulation and analyzed by analytic approximations. The results are in good agreement with the measured energy gap of $(GaAs)_{1-x}Ge_{2x}$ and with the results of x-ray, Raman, and extended x-ray-absorption fine-structure determinations of the order parameter and the nearest-neighbor environments in $(GaSb)_{1-x}Ge_{2x}$. We also present calculations of the, as yet unreported, energy gap of the latter compound.

I. INTRODUCTION

Thin films of pseudobinary alloys of III-V compound semiconductors with germanium have been made by Greene and co-workers,[1-4] who used a modified sputtering technique and by others using metalorganic chemical-vapor deposition (MOCVD)[5] or molecular-beam epitaxy (MBE).[6] Here we will be concerned with the alloys $(GaAs)_{1-x}Ge_{2x}$ and $(GaSb)_{1-x}Ge_{2x}$, both of which are metastable. From a theoretical standpoint the alloy of Ge with GaAs is the more attractive because its components have almost identical lattice constants and their bonding should be quite similar. Also its optical energy gap is known to be in a range (0.5—1.5 eV) that is potentially useful for optoelectronic devices,[3] although no such device has yet been reported. However, the available experimental data for $(GaAs)_{1-x}Ge_{2x}$ are far from adequate for a complete characterization and we must supplement them with measurements of the related $(GaSb)_{1-x}Ge_{2x}$.

An understanding of the factors that lead to the observed deep bowing of the energy-gap—versus—composition curve of $(GaAs)_{1-x}Ge_{2x}$ is particularly desirable. A further feature of interest is the transition between the zinc-blende and diamond symmetries of the two constituents that perforce occurs at some composition. Here one would like to understand the composition dependence of the ordering of the diamond lattice into the two interpenetrating fcc sublattices that comprise the zinc-blende structure. In particular, any satisfactory theory of the alloys must predict correctly the critical mole fraction of Ge, x_c, above which this ordering vanishes. Finally we need to consider the statistics of the nearest-neighbor (NN) relationships. These are important because, to the extent that a tight-binding approximation is valid, they dominate the distribution of electronic energy states, and hence the energy gap, to the virtual exclusion of the effects of longer-range ordering.

Calculations of the structure and the direct energy gap of $(GaAs)_{1-x}Ge_{2x}$ were made by Newman and Dow[7] (ND) who applied a three-component spin model to the NN interactions. This led to a composition-dependent ordering in response to a postulated local minimum in the free energy of the metastable alloy. Lacking a calculation for x_c, they derived a composition dependence of the order from the speculation that x_c is also associated with the minimum energy gap, i.e., that $x_c \approx 0.3$. The virtual-crystal approximation (VCA) was then used to obtain a composition dependence of the energy gap that was in fair agreement with the rather scattered experimental data. (Later studies[8] extended the calculations to similar alloys for which there are no experimental data.) However, subsequent work by Holloway and Davis,[9,10] showed that these calculations were erroneous because the VCA is not valid for $(GaAs)_{1-x}Ge_{2x}$. In fact, application of the more accurate Haydock recursion method to clusters with the same NN statistics as the mean-field theory used by ND gave zero energy gap for midrange compositions, rather than the observed value of about 0.5 eV. This difference arises because the VCA, from its nature as an average of the components, is inherently incapable of handling strong alloy scattering. This arises in the ND model from large concentrations of As—As NN pairs. In particular, the model implies complete randomness of Ga and As site occupancy when $x > x_c$. (An equal concentration of Ga—Ga NN pairs is also implied, but these have less effect on the energy gap.) This leads to VCA-derived energies for the lowest conduction band with errors that are larger than the energy gap of the alloy.[11]

From comparison of our calculations with experimental values of the direct energy gap we concluded that Ga—Ga and As—As NN pairs do not occur in $(GaAs)_{1-x}Ge_{2x}$. (Even moderate concentrations of As—As NN pairs caused the gap to vanish. A refinement of the ND model by Koiller *et al.*[12] decreases the As—As NN-pair concen-

tration, but not by enough to remove this difficulty.) We then incorporated this conclusion into a statistical model of the alloy structure[9] that has since become known as the percolation model. This did not involve a cooperative ordering phenomenon of the kind proposed by ND. Instead the lattice sites were occupied randomly, subject to the restrictions that wrong NN pairs were prohibited and that the GaAs component occurred as Ga—As NN pairs. (Most subsequent theory for the alloy, including that presented here, resembles the percolation model by postulating random site occupancy subject to some NN restrictions.) Our percolation model gave an energy gap that was in acceptable agreement with experiment and it also predicted a rather large critical composition, $x_c=0.75$. (Note that this was an absolute prediction because, unlike ND, the percolation model does not contain any adjustable parameters.)

Recently Shah *et al.*[13] used x-ray diffraction to obtain the first direct evidence of an order-disorder transition in $(GaSb)_{1-x}Ge_{2x}$. The (002) reflection, which is allowed in the zinc-blende structure, but forbidden in the diamond lattice, was found to disappear as x increased from zero to 0.3. This implies that, at larger Ge contents, each fcc sublattice of the zinc-blende structure contains equal concentrations of Ga and Sb atoms, corresponding to diamond symmetry. (The interpretation is subject to the limitation that x-ray measurements average over distances of the order of microns, so that ordering on a smaller scale would not be detected.) The observed value of $x_c=0.3$ is much smaller than that predicted by our percolation model, but it agrees with the value inferred for $(GaAs)_{1-x}Ge_{2x}$ by ND. Less direct evidence for a phase transition can also be seen in the Raman spectra of $(GaSb)_{1-x}Ge_{2x}$.[14–17] [Similar x-ray measurements of $(GaAs)_{1-x}Ge_{2x}$ are difficult because the constituent atoms have almost equal scattering factors.[13]]

Later extended x-ray-absorption fine-structure (EXAFS) measurements of $(GaSb)_{1-x}Ge_{2x}$ by Stern *et al.*[18] showed an absence of Ga NN's around the Ga atoms. This agrees with the absence of wrong NN pairs in our percolation model. [As with x-ray experiments, the small differences between the constituent atoms make EXAFS difficult with $(GaAs)_{1-x}Ge_{2x}$.] Interpretation of the Raman spectra of $(GaSb)_{1-x}Ge_{2x}$ is subject to some uncertainty, but again there is no evidence for the Ga—Ga and Sb—Sb NN pairs that are predicted by the ND theory.[19] Unfortunately, despite the theoretical importance of $(GaSb)_{1-x}Ge_{2x}$, we lack information about its energy gap.

In the next round of refinement Kim and Stern[20] (KS) proposed a model in which growth of $(GaAs)_{1-x}Ge_{2x}$ was simulated layer by layer. Site occupancy was subject to prohibition of Ga—Ga and As—As NN pairs. This process resembled our implementation of the percolation model,[21] but new ground was broken by recognizing that the sequence in which the lattice sites are filled defines a direction for simulated growth. Pairing of Ga and As atoms was not imposed and, consequently, stoichiometry was achieved only by assuming identical behavior of Ga and As. (Under real growth conditions these constituents have significantly different volatilities and concentrations.) Nevertheless, the calculated $x_c=0.26$ for $\langle 100\rangle$ growth is remarkably close to the experimental value for $(GaSb)_{1-x}Ge_{2x}$. (As in the percolation model, x_c is not an adjustable parameter here.) KS also suggested that different growth directions could give different values of x_c (from the results of a simulation of growth spherically outward from a single atom). In contrast to the relative success of the KS model with $\langle 100\rangle$ growth, attempts to simulate $\langle 111\rangle$ growth gave unrealistic model lattices with large concentrations of Ge atoms on alternate $\{111\}$ planes.

In the present paper we introduce a new theory for the structure of $(GaAs)_{1-x}Ge_{2x}$. This we designate the growth model. We retain the short-range order (SRO) that was imposed by the NN restrictions of the percolation model and thereby also retain a good fit to the energy gap. However, the long-range order (LRO) now arises from a set of rules for adding atoms to the growing surface. These rules are physically reasonable for growth of $(GaAs)_{1-x}Ge_{2x}$ and they may also apply to growth of $(GaSb)_{1-x}Ge_{2x}$.

The model has been implemented by Monte Carlo (MC) simulation of crystal growth in the $\langle 100\rangle$ direction, which corresponds to that used experimentally for growth of the alloys. We will show that the resulting structures reproduce the known properties of $\langle 100\rangle$ grown alloys, including the energy gap of $(GaAs)_{1-x}Ge_{2x}$ and the order parameter of $(GaSb)_{1-x}Ge_{2x}$ (with its transition at $x_c=0.3$). Further confidence in the realism of the growth model arises from the insensitivity of its results to variations in the details of its implementation. Indeed we find that the most important results of MC simulations are reproduced by an even simpler analytic approach that neglects all except NN correlations.

Calculations of the energy gap of $(GaAs)_{1-x}Ge_{2x}$ with the statistical structure that arises from our new model gave results similar to those from the structure defined by our earlier percolation model. This accords with our assertion that the gap is dominated by the SRO. However, we have also investigated the refinement of our previous recursion calculations by the inclusion of d, as well as s and p, orbitals. This allows better fitting of the conduction bands of the pure components and it gives better agreement with the experimental gap for the alloy, but it does not greatly affect our previous conclusions about the gap of this material. (Neither does it affect our conclusions about the consequences of the VCA-related error in the ND calculations. Even after refinement by inclusion of d orbitals, the recursion method still indicates that the lattice statistics of the ND model would lead to zero gap at compositions near the middle of the range.) We also include here a prediction of the energy gap of $(GaSb)_{1-x}Ge_{2x}$ that is based on the recursion method.

II. THE GROWTH MODEL

In this section we introduce a new model for $(GaAs)_{1-x}Ge_{2x}$ and related alloys. This is based on the postulate that the structure of the alloy is determined by a stochastic growth process in which, first, As (in one form or another) is always present in large enough excess to

react with any free Ga on the surface and, secondly, the substrate temperature is high enough to reevaporate any unreacted As. These conditions appear to be consistent with published descriptions of the growth of $(GaAs)_{1-x}Ge_{2x}$. Moreover, to the extent that excess Sb is used at high enough growth temperatures, they may also apply to $(GaSb)_{1-x}Ge_{2x}$. For convenience, the following discussion refers specifically to Ga and As, but the arguments may also be applicable to other pairs of elements from groups III and V.

The conditions used for implementation of our model are listed below. Several of them include optional variations that we used to test the sensitivity of the results to details of the implementation. In subsequent discussion we shall refer to the "simple" implementation as that without any of the variations. Also, since we will be considering layer-by-layer growth, it will be convenient to refer to the lattice plane whose vacant sites are being filled randomly by Ge or Ga atoms as the "current" plane. The corresponding just-filled and about-to-be-filled planes are termed "preceding" and "following" planes, respectively.

(1) Epitaxial growth is initiated on a {100} lattice plane of a GaAs substrate. This orientation has been chosen to correspond to published growth conditions. (Preliminary studies indicate that the results are strongly dependent on substrate orientation.[22])

Examination of the crystal structure of pure GaAs (Fig. 1) shows that the occupancy of successive {100} planes alternates between all Ga atoms and all As atoms. We assume that growth starts on a {100}As plane. This is probably realistic because in the presence of a large excess of As [see (2) below] a {100}Ga plane would be covered by As atoms before significant alloy growth could occur.

(2) Layer-by-layer growth of the alloy is simulated by filling vacant sites on successive lattice planes with a random choice of either Ge or Ga atoms. Within each plane the vacant sites are filled in random sequence. When a Ga atom is added it reacts immediately with an As atom, which then occupies an NN site on the following plane. (This is the only mechanism for incorporation of As into the alloy.) In this procedure we neglect the possible influence of surface reconstruction.

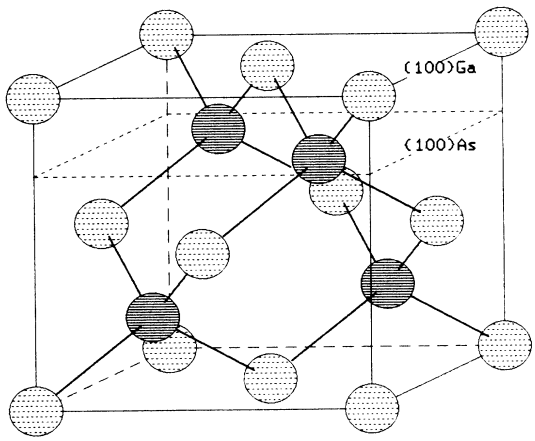

FIG. 1. Unit cell of the zinc-blende structure showing alternating {100} layers of the two constituents. Note also the connection of each atom to two NN's in each of the preceding and following {100} planes.

Published descriptions of $(GaAs)_{1-x}Ge_{2x}$ growth generally indicate the presence of a significant excess of As, of which only enough is incorporated to maintain approximate stoichiometry of the GaAs constituent. Our postulated addition of GaAs as molecules appears to be the simplest way to achieve this result. (Individual Ga and As atoms may dissolve in Ge to a much smaller extent, to act as acceptor and donor impurities, respectively.)

(3) The addition of a Ga atom is subject to the condition that it does not create either a Ga—Ga or an As—As NN pair. (We note that Ga—Ga and As—As or Sb—Sb NN pairs are rare in pure GaAs and GaSb and that, from the evidence cited in Sec. I, the existence of significant concentrations of these wrong NN's in the alloys is unlikely.)

At each vacant site the decision to add a Ge atom is made definitely with a predetermined probability P_{Ge}. The alternative decision, to add a Ga atom (with an NN As atom on the following {100} plane) will then occur with the complementary probability $1-P_{Ge}$. However, in this case the decision is tentative and the Ga addition is only made after confirming that it will not give undesired NN pairs. If addition of a Ga—As atom pair would violate an NN restriction, a Ge atom is added instead. (Such forced addition of Ge is similar to that encountered in the KS model, although its consequences are nowhere near so large here. However, it does give rise to a composition parameter, x, that differs somewhat from P_{Ge}.)

In an optional variation these NN restrictions are relaxed at the boundaries between GaAs clusters with the phase and antiphase orientations (as defined in Sec. III). This amounts to allowing a Ga (or As) atom to have an otherwise forbidden Ga (or As) NN if it also has at least one As (or Ga) NN. The variation avoids the forced incorporation of Ge at domain boundaries.

(4) A Ga atom that arrives at an unsuitable site reevaporates and the site is filled with a Ge atom instead. This assumption is not entirely realistic because Ga adatoms on the alloy surface might be expected to have significant surface mobility and limited volatility at typical growth temperatures (450—750 °C). (Reevaporation of unwanted Ga is also assumed by KS.) However, approximate modeling of these effects, described next, shows that they have negligible influence upon the results.

In a variation we allowed Ga atoms to make a random walk across the surface in search of a suitable site. Here, if a site was found to be unsuitable for a Ga atom it was filled, as before, with a Ge atom. The unwanted Ga atom was then reevaporated with a predetermined probability. (We used an arbitrarily chosen value of 0.1.) If the Ga atom did not reevaporate an attempt was then made to place it on a randomly chosen adjacent site in the current plane. From here, if the site was occupied a further choice was made between reevaporation and a random move, otherwise the new vacant site was checked for suitability as if the Ga atom had arrived there by direct

choice of the site. The process continued until the Ga atom either reevaporated or found a suitable lattice site.

The variation approximates a situation with Ga adatoms that are mobile and relatively involatile, although it is somewhat unrealistic in two ways. First, the restriction to movement between sites on the current plane does not allow for the possibility that the Ga atom might cross the As atoms of the following plane to find a suitable site on a later {100}Ga plane. This could lead to surface roughening with simultaneous growth on many {100} planes. Second, the filling of an unsuitable site with a Ge atom immediately (rather than upon random arrival of a Ge atom) reduces the extent to which such a site acts as a source of Ga for the surrounding surface. However, we found that the lattice statistics obtained with this first approximation to the behavior of mobile Ga adatoms did not differ significantly from those with the simpler assumption of complete reevaporation from unsuitable sites. Consequently, we did not attempt to refine the approximation (or even to explore the effect of varying the reevaporation probability).

(5) The simulation created a succession of {100} lattice planes that were bounded by {110} planes that were orthogonal to them. We assumed that the sample was periodic across these {110} boundaries. Periodicity was imposed for two reasons. First, in the recursion calculation of the electronic states the cluster sizes are relatively small. Here the periodicity eliminates errors that could arise from wrong NN relationships across the bounding planes because the recursion calculation applies periodic boundary conditions to the sample cluster of atoms. (In the present case we have eliminated the wrong NN's across bounding {110} planes, but some will still occur across {100} bounding planes. However, comparison with calculations for the previous percolation model, where wrong NN's were eliminated from both {110} and {100} boundaries, shows that the resulting errors are small.) Secondly, the periodic boundary conditions allowed us to approximate the addition of atoms to an infinite lattice plane that is partly filled.

In a variation of the simple implementation the periodic boundary conditions were eliminated. Here, NN sites outside the {110} boundaries of the sample were assumed to be vacant, thereby not contributing to restrictions on sites occupancy. This was done to test the dependence of the observed structure on the relative smallness of the samples perpendicular to the growth direction. Our concern was that population choices along the boundaries might have a disproportionate effect because they affect NN relationships on two sides of the sample. The variation eliminated this effect at the cost of introducing some sites that had fewer NN restrictions than those in a real crystal.

III. NUMERICAL RESULTS AND COMPARISONS WITH EXPERIMENT

For our discussions of LRO we define the "phase" orientation of the GaAs constituent of $(GaAs)_{1-x}Ge_{2x}$ to be that with its Ga and As atoms occupying the same sets of alternate {100} planes as the Ga and As atoms of the GaAs substrate. We may then define an antisite fraction, f, of the alloy as the fraction of the GaAs constituent that is in the alternative "antiphase" orientation. Possible values of f range from zero, for the fully ordered zinc-blende lattice, to 0.5 for the completely disordered diamond lattice. ($f=1.0$ for a fully ordered zinc-blende lattice with the antiphase orientation.) The antisite fraction may be related to an order parameter, M, (defined equivalently to that of ND) by

$$M=(1-x)(1-2f) . \tag{1}$$

It is also helpful to have a simple measure of the sizes of the continuous clusters or domains of Ge and GaAs (both phase and antiphase) that occur within a sample of the alloy. For this purpose we associate with each atom of the sample a length l that we define as the number of layers that may be reached from the atom by traveling to preceding layers via NN atoms of the same domain. (From Fig. 1 we can see that each site on a {100} plane has two NN's on the preceding plane plus two NN's on the following plane.) For Ge atoms we will always travel via other Ge atoms, but for Ga or As atoms we will trace a path via alternate Ga and As atoms with opposite sequences for phase and antiphase domains. Our measure of the domain size in the growth direction is then the average of this length, $\langle l \rangle$, over all of the atoms of the appropriate type within the sample. Clearly, as a component's concentration becomes large enough we will get $1/\langle l \rangle \rightarrow 0$, corresponding to a domain with infinite depth. The concentration at which this occurs resembles a percolation threshold for the growth direction. However, our clusters will be smaller than those usually considered in percolation theory because we do not count cluster members that might be reached by a combination of backward and forward moves through the sample. Thus the onset of infinite cluster depth for a component, as measured here, sets an upper bound for the conventional percolation threshold. (In fact, as discussed later, the restriction to moves in one direction through the sample gives a situation akin to percolation on a tree.) Nonetheless, our definition of $\langle l \rangle$ does give a useful and readily calculable measure of domain size. Particularly, the MC simulations are simplified and made capable of extension to very large samples because we need to keep track of the occupancy of the sites on only three successive planes and of the values of l on only two planes.

Growth simulations were carried out using {100} planes that ranged from 10×10 to 50×50 atoms (along $\langle 110 \rangle$ directions orthogonal to the growth direction) with most of the work being done at 20×20 and 50×50 atoms. Very little dependence of the results upon the size of the cross section was found although, as might be expected, the smaller specimens gave larger fluctuations in the lattice statistics. To ensure attainment of a steady state, at least 1000 planes were grown before beginning the averaging of sample properties and in some cases even longer lead-ins were made. The averages were mostly of 2000 planes, although overall we used 500—6000 planes. The adequacy of the lead-ins for establishing constant lattice statistics was verified by inspection.

At this stage we first give the results of the "simple"

implementation of the growth model and compare them to the available data for the LRO and the NN statistics. We will then consider briefly the effects of variations in the implementation.

Figure 2 shows the composition dependences of $1/\langle l \rangle$ for the Ge component and the phase and antiphase GaAs components that we obtained from MC calculations using the "simple" implementation. These results subdivide the composition range into four regions as follows.

(1) When Ge is added to GaAs we first pass through a range ($x \lesssim 0.31$) where the alloy, with zinc-blende symmetry, has an infinite domain of the GaAs phase component. With increasing Ge content the antiphase GaAs component increases its concentration and its domains, though finite, have increasing average size.

(2) With $0.31 \lesssim x \lesssim 0.42$ we pass through a small range in which both the phase and antiphase orientations of GaAs exhibit infinite domains. At a little after the beginning of the region ($x \approx 0.34$) the zinc-blende order (as an average over the whole specimen) disappears to leave, as a residue, diamond symmetry.

(3) Next we find a region ($0.42 \lesssim x \lesssim 0.56$) where the domains of all three components are finite.

(4) Finally, with $x \gtrsim 0.56$, the domains of both GaAs orientations are finite, but the Ge component has an infinite domain.

The second region, with $0.31 \lesssim x \lesssim 0.42$, is particularly interesting because LRO persists in both phase and antiphase domains of the GaAs component, despite the zero value of the order parameter that pertains to the specimen as a whole over most of this composition range. No other theory of the present alloys has predicted such an ordering and, to our knowledge, the effect has not been explored with other alloy systems. Averaging over the specimen is appropriate for the order parameter as determined by x-ray diffraction because our simulations yield phase and antiphase domains that are mixed on a scale that is small by comparison with x-ray extinction distances that are typically a few μm. Images of our MC grown crystals with compositions in region 2 show that the phase and antiphase domains coexist within {100} planes that have dimensions in the range 20×20 to 50×50 atoms and that each of these domains tends to remain connected for thousands of consecutive {100} planes.[23]

The prediction of interpenetrating infinite zinc-blende domains in a specimen whose average order is that of diamond is intriguing, although it may be difficult to verify experimentally. We think it likely that this result is realistic, rather than an artifact of our MC simulation, because we obtained the same prediction from an analytic approximation that is described in Sec. IV. This rules out explanations in terms of artifacts that are due to the limited size of our {100} sample plane. (Similar evidence is provided by persistence of the result when we remove the periodic boundary conditions.)

Figure 3 shows the composition dependence of the order parameter calculated from the "simple" implementation together with experimental data for $(GaSb)_{1-x}Ge_{2x}$ from Shah *et al.*[13] Clearly, the agreement is excellent. Our MC simulations give $x \approx 0.34$ compared with the experimental value of $x_c = 0.30$–0.31.

In Figs. 4 and 5 we show the number of group V NN's of Ga and of Ge atoms obtained from the same MC simulations. (The simple implementation gives NN environments in which Ge atoms have equal numbers of group III and group V NN's and in which the number of group III NN's of a group V atom is equal to the number of group V NN's of a group III atom.) Here we are able to make a comparison with data from Stern *et al.*[18] for the number of Sb NN's around Ge and Ga atoms in $(GaSb)_{1-x}Ge_{2x}$. For the Ga environment the agreement

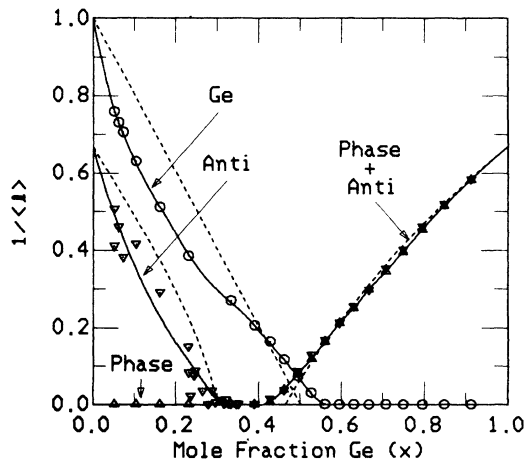

FIG. 2. Reciprocal average length ($1/\langle l \rangle$) of the Ge and the phase and antiphase GaAs components of $(GaAs)_{1-x}Ge_{2x}$. The symbols and the solid lines are from the MC growth simulations and the dotted lines are the analytic approximations.

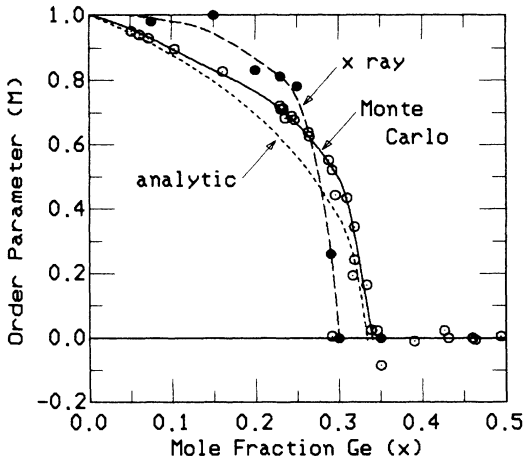

FIG. 3. Composition dependence of the order parameter. The open circles and the solid line are from the MC simulation. The dotted line is the analytic approximation. The solid circles and the dashed line are the results of x-ray measurements by Shah *et al.* (Ref. 13).

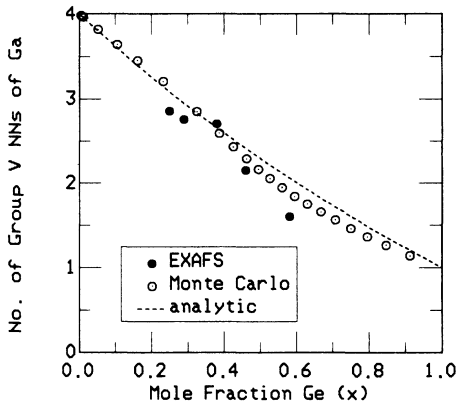

FIG. 4. Composition dependence of the number of group V NN's of a Ga atom in the alloys. The open circles are the MC results and the dotted line is the analytic approximation. The solid circles are EXAFS results for Sb NN's in $(GaSb)_{1-x}Ge_{2x}$ by Stern *et al.* (Ref. 18).

with theory is excellent.[24] In the case of the Ge environment the data for N_{Sb} are about 30% lower than our calculations. (In this case the calculated N_{Sb} versus x does not exhibit much curvature. Stern *et al.*[18] suggested that this deviation from the expected relationship arose from preferential substitution of Ge atoms at Sb sites that are associated with imperfections.)

At this stage we note an effect of the finite size of our sample {100} planes. In the limit of vanishingly small concentrations of Ge atoms that are randomly distributed on the sites of a III-V compound that has a zinc-blende lattice we will average over equal numbers of Ge atoms with either four group III NN's or four group V NN's. Thus, we should expect Fig. 5 to show an average of two group V NN's when $x \rightarrow 0$. Instead we get an intercept at about 1.9 group V NN's. This is an indirect consequence of our pairing of group III and group V atoms in a finite sample. Each $N \times N$ {100} plane of our sample consists of N rows of N atoms along ⟨110⟩ directions that are orthogonal to the ⟨100⟩ growth direction. Consider the region where $x \rightarrow 0$. The act of placing a Ge atom on one of the sites along a ⟨110⟩ row of a {100}Ga plane reduces by one the number of NN As atoms in the ⟨110⟩ row of the following {100}As plane. Since Ga—Ga NN pairs are forbidden, the vacant site on the following ⟨110⟩ row is then forced to also contain a Ge atom. Since each site has two NN's on the following ⟨110⟩ row, these pairs of Ge atoms that are implied by our NN pairing of Ga and As have $2/N$ probability of being NN's themselves when the Ge concentration is small. Thus, the finite-size effect would be expected to give $2/N$ Ge NN's of a Ge atom in this limit. The data in Fig. 5 were obtained with $N=20$ and this accounts for the discrepancy of about 0.1 in the average number of group V NN's at $x=0$. We have also observed appropriate size effects with other sample sizes.

Next we consider the effects of varying the details of the growth simulation as described in Sec. II. Evaluation of the dependences of $1/\langle l \rangle$ upon x showed that neither the elimination of the periodic boundary conditions nor the inclusion of limited reevaporation and random walks for Ga adatoms had much effect on the results, which remained close to those of the "simple" implementation that are shown in Fig. 2. Significant changes did occur when we allowed wrong NN's to exist at the boundaries between phase and antiphase domains. In particular the order-disorder transition was moved from $x_c \approx 0.3$ to $x_c \approx 0.2$. However, this variation was found to give significant numbers of wrong NN's, as shown in Fig. 6. Particularly, at mid-range compositions the As atoms average about $\frac{1}{2}$ of an As NN each. Our recursion-method calculations using the sp^3s^* model described in Sec. V have shown that such concentrations of As—As NN pairs are inconsistent with the energy gap of $(GaAs)_{1-x}Ge_{2x}$ and

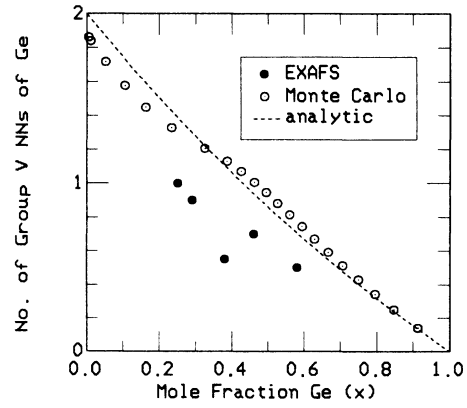

FIG. 5. Composition dependence of the number of group V NN's of a Ge atom in the alloys. The open circles are the MC results and the dotted line is the analytic approximation. The solid circles are EXAFS results for Sb NN's in $(GaSb)_{1-x}Ge_{2x}$ by Stern *et al.* (Ref. 18).

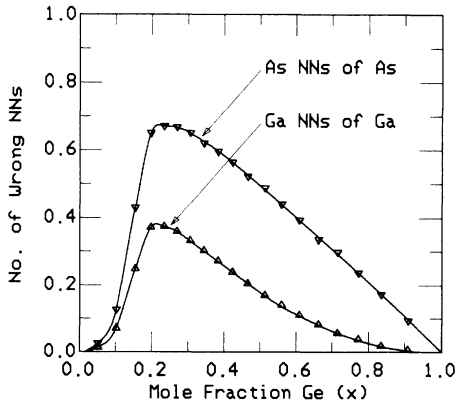

FIG. 6. Composition dependences of the number of wrong NN's (As around As and Ga around Ga) from MC simulations that allowed wrong NN's at the boundaries between phase and antiphase domains.

therefore we abandoned this variation as unrealistic. (Essentially the effect of As—As NN pairs here is to close the gap in the same way as described previously for the ND model.[9,10])

Finally, we consider the relationship between the present growth model and our earlier percolation model. In our earlier work[9] we attempted to populate a diamond lattice with a random mixture of Ge atoms and diatomic GaAs molecules. One cannot reach the whole composition range by filling the sites in random sequence because, with increasing population, one will reach a situation where the remaining vacant sites are isolated and thereby incapable of accepting the diatomic constituent. (This is the well-known "parking" problem.) To avoid the problem we populated the lattice on successive {100} planes, as in the present model. (This point was omitted in our previous letter.[9]) The process has obvious similarities to both the present growth model and the KS growth simulation.

The main difference between the growth model and the percolation model arises because in the latter we used MC methods to generate samples of the crystal lattice that were small enough (up to 4096 atoms) to permit evaluation of conventional percolation statistics with the aid of a small computer. We assumed implicitly that any infinite cluster of the GaAs component would dominate the LRO and thereby overlooked the possibility of simultaneous occurrence of infinite clusters of the phase and antiphase components of GaAs. This neglected possibility was subsequently made obvious by the results of the present growth simulations where a change in the definition of cluster dimension (to $\langle l \rangle$) allowed the evaluation of samples with up to about 10^7 atoms. (Clearly, interpenetrating infinite three-dimensional networks can exist as, for example, with the pores and the body of a sponge.)

With this difference in mind we may make a crude estimate of the values of x_c that will be given by the two methods. Let us assume that any component on a diamond lattice will percolate at a critical concentration in the range $p_c=0.3$–0.4. (For simple substitution on the diamond lattice $p_c=0.4$, but we obtain a somewhat smaller value for a diatomic constituent.) Then the percolation model identifies the order-disorder transition with the onset of percolation of the diatomic constituent of a monatomic-diatomic mixture, so that $x_c=1-p_c \approx 0.6$–0.7. In contrast, the growth model suggests that the transition occurs near the onset of simultaneous percolation by the phase and the antiphase GaAs components to give $x_c=1-2p_c \approx 0.2$–0.4. These values cannot be regarded as more than suggestive. (In particular, our application of an isotropic percolation threshold to infinite domains in the growth direction is imprecise.) Nevertheless, they are similar to those (0.75 and 0.3, respectively) that are given by the two MC approaches.

IV. AN ANALYTIC MODEL

In this section we derive analytic approximations for the stochastic growth process that was described in Sec. II. While we will sacrifice accuracy relative to the MC simulation, we will be able to confirm its major features and gain some insight into their origins.

Let $p(n)$ be the probability that a site in the nth layer beyond the substrate is occupied by a Ga atom, $q(n)$ the probability of occupancy by an As atom, and $x(n)$ by a Ge atom. To calculate the probability that a site in the $(n+1)$th layer is occupied by a Ga atom, we must consider its two NN sites in layer n. If one or both of these underlying NN sites is occupied by a Ga atom, the present site cannot contain a Ga atom. Neglecting in-plane correlations, the probability that the two underlying NN sites contain no Ga atoms is $[q(n)+x(n)]^2=[1-p(n)]^2$. Therefore, if we also neglect the NN restrictions on the companion As atom, the probability that a site in layer $n+1$ is occupied by a Ga atom is

$$p(n+1)=(1-P_{\mathrm{Ge}})[1-p(n)]^2 . \tag{2}$$

The initial condition is $p(0)=0$ since we are growing from the As surface of a GaAs substrate.

For large n, steady state is approached. Let us look for solutions appropriate to the zinc-blende structure: $p(n)=p(n+2)=\cdots=p_2$, $p(n+1)=p(n+3)=\cdots=p_1$. Then

$$p_1=(1-P_{\mathrm{Ge}})(1-p_2)^2 , \tag{3a}$$

and

$$p_2=(1-P_{\mathrm{Ge}})(1-p_1)^2 . \tag{3b}$$

If we assume that $p_1 \neq p_2$ we obtain the solutions

$$p_1=[1-2P_{\mathrm{Ge}}+(1-4P_{\mathrm{Ge}})^{1/2}]/2(1-P_{\mathrm{Ge}}) \tag{4a}$$

and

$$p_2=[1-2P_{\mathrm{Ge}}-(1-4P_{\mathrm{Ge}})^{1/2}]/2(1-P_{\mathrm{Ge}}) . \tag{4b}$$

Since $q(n+1)=p(n)$ (because of Ga—As pairing), the As composition on layer $n+1$, $n+3$, . . . , is $q_2=p_1$ and on alternate layers $q_1=p_2$. Consequently, the Ge composition is the same in each layer:

$$x=1-p_1-p_2 \tag{5a}$$

$$=P_{\mathrm{Ge}}/(1-P_{\mathrm{Ge}}) . \tag{5b}$$

Another solution to Eq. (3) is

$$p_1=p_2$$

$$=[3-2P_{\mathrm{Ge}}-(5-4P_{\mathrm{Ge}})^{1/2}]/2(1-P_{\mathrm{Ge}}) . \tag{6}$$

[In Eq. (6) we neglect an unphysical solution that gives $p_1,p_2>1$.] The Ge concentration $x=1-2p_1$ is

$$x=[P_{\mathrm{Ge}}+(5-4P_{\mathrm{Ge}})^{1/2}-2]/(1-P_{\mathrm{Ge}}) . \tag{7}$$

The results of Eqs. (4) and (6) are shown in Fig. 7. Note that the values given by Eqs. (4) remain real with increasing P_{Ge} until $P_{\mathrm{Ge}}=\frac{1}{4}$. At this point we have $p_1=p_2=\frac{1}{3}$, i.e, the the zinc-blende order must disappear at $x_c=1-p_1-p_2=\frac{1}{3}$. This is in excellent agreement with both the experimental value of about 0.31 and the value of about 0.34 from the MC simulation.

So far we have ignored the solution with $p_1=p_2$ in the region where $P_{\mathrm{Ge}}<\frac{1}{4}$. A simple argument shows that this solution is unstable there. Suppose that the $(n+1)$th

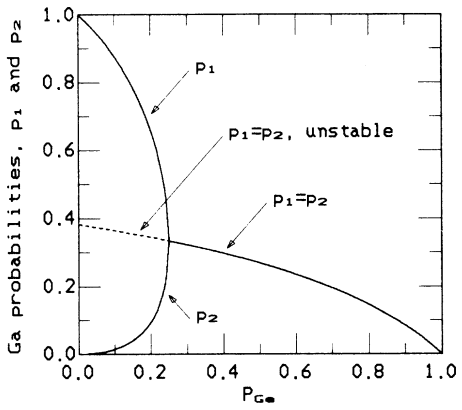

FIG. 7. Analytic approximations for the phase and antiphase GaAs concentrations (p_1 and p_2) as functions of P_{Ge}. The solution with $p_1=p_2$ and $P_{Ge}>0.25$ corresponds to diamond symmetry. Note that the actual Ge concentration x differs from P_{Ge}.

plane is {100}Ga with a nonsteady state Ga atom concentration of

$$p(n+1)=p_1+\delta_{n+1} \tag{8}$$

and that this is preceded by a {100}As plane with a nonsteady state Ga atom concentration of

$$p(n)=p_2+\delta_n\ , \tag{9}$$

where $|\delta_{n+1}/p_1|, |\delta_n/p_2| \ll 1$. From Eq. (3), we find

$$\delta_{n+1}=-2(1-P_{Ge})(1-p_2)\delta_n \tag{10}$$

and

$$\delta_n=-2(1-P_{Ge})(1-p_1)\delta_{n-1}\ . \tag{11}$$

Since $P_{Ge}, p_1, p_2 \le 1$, the deviations from the solutions given by Eqs. (4) and (6) must alternate in sign as we add successive layers. Now suppose that we are close to a solution with $p_1=p_2$, as given by Eq. (6). In this case

$$\begin{aligned}|\delta_{n+1}/\delta_n| &=[(5-4P_{Ge})^{1/2}-1] \\ &> 1 \text{ when } P_{Ge}<\tfrac{1}{4}\ , \\ &< 1 \text{ when } P_{Ge}>\tfrac{1}{4}\ .\end{aligned} \tag{12}$$

Thus, the solution with $p_1=p_2$ is stable only when $P_{Ge}>\frac{1}{4}$.

If instead we are close to one or the other of the solutions with $p_1 \neq p_2$, as given by Eqs. (4), we need to consider the change in δ that occurs as we reach successive {100}Ga or {100}As planes, respectively. From Eqs. (4), (10), and (11) this is given, for either kind of {100} plane, by

$$\delta_{n+1}/\delta_{n-1}=4P_{Ge}\ , \tag{13}$$

which gives stability when $P_{Ge}<\frac{1}{4}$, i.e., over the range where real solutions of Eq. (4) exist and where the solution of Eq. (6), with $p_1=p_2$, is unstable.

The approach of $p(n)$ to steady state in the region where $P_{Ge}<\frac{1}{4}$ is illustrated in Fig. 8. Here $P_{Ge}=0.1$ and the unstable solution given by Eq. (6) has $p_1=p_2=0.364$. Starting with $p(0)=0.36$ and applying Eq. (2), we find that with successive layers, $p(n)$ undergoes an oscillation that increases until, after about 45 layers, we attain the steady-state values given by Eqs. (4), i.e., $p_1=0.875$ and $p_2=0.014$. If instead we start with $p(0)=0$ or $p(0)=1$, we reach the steady-state solution after only about ten layers. The different behavior when $P_{Ge}>\frac{1}{4}$ is shown in Fig. 9. Here we have $P_{Ge}=0.4$ and the only steady-state solution is $p_1=p_2=0.297$, which is seen to persist as we add layers. If instead we start with $p=0$ or $p=1$, the steady-state value is reached after about 30 layers.

Since the antisite fraction at steady state is

$$f=p_2/(p_1+p_2)\ , \tag{14}$$

it follows from Eq. (1) that the order parameter may also be expressed as

$$M=p_1-p_2\ . \tag{15}$$

Using values of p_1 and p_2 from Eqs. (4), we obtain the composition dependence of the order parameter that is shown as a dotted line in Fig. 3. In addition to the good agreement of $x_c=\frac{1}{3}$ with the MC value, upon which we have already commented, we note that at other values of x the curve is also reasonably close to that derived by MC simulation.

We now obtain analytic approximations for the values of $\langle l \rangle$ that are associated with the Ge and GaAs clusters. As noted earlier, the unidirectionally connected clusters that are measured in our determination of $\langle l \rangle$ are similar

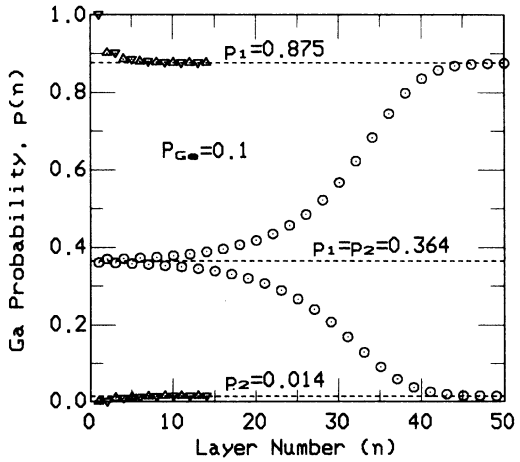

FIG. 8. Analytic approximation for the evolution of the Ga concentration $p(n)$ into the phase and antiphase concentrations (p_1 and p_2) with growth of successive {100} layers in the region with zinc-blende symmetry ($P_{Ge}=0.1$). The circles show the divergence from a value ($p=0.36$) that is close to the unstable solution with $p_1=p_2$. The two orientations of triangle show the evolution of p_1 and p_2 from initial values of zero and unity, respectively.

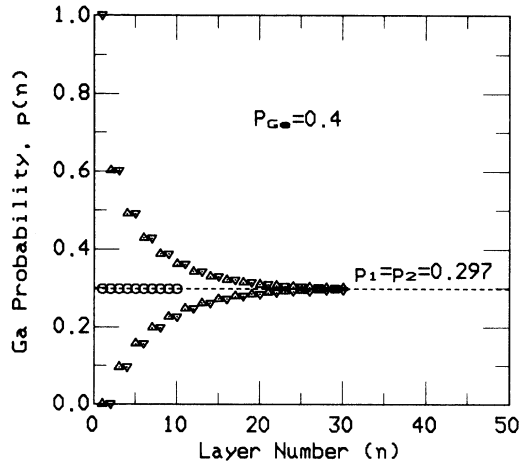

FIG. 9. Analytic approximation for the evolution of the Ga concentration $p(n)$ into equal phase and antiphase concentrations ($p_1=p_2$) with growth of successive {100} layers in the region with diamond symmetry ($P_{Ge}=0.4$). The circles show the stability of the solution with $p_1=p_2=0.297$. The two orientations of triangle show the convergence to this solution from initial values of zero and unity, respectively.

to those that would be generated by substitution on a tree. In the following we approximate the diamond lattice by a uniformly branched tree in order to gain tractability. Thus, as we follow a cluster down a ⟨100⟩ axis we will assume that the two underlying NN's of each cluster member are not associated with any other path downwards through the specimen, i.e., that the potentially connected sites of a given site increase in the sequence 2,4,8,16, . . . , as we reach successive underlying {100} planes. Inspection of Fig. 1 shows that the numbers actually increase more slowly, i.e., as 2,4,6,9, . . . , . Thus, if we work downwards with a single atom, at large concentrations of a component we will overestimate the number of connected atoms on an underlying plane. However, our cluster size, $\langle l\rangle$, becomes infinite when the expected number of connected atoms in underlying planes exceeds unity. Hence our approximation is reasonable for finite clusters.

Consider first a uniformly distributed monatomic constituent on a tree. Let the probable number of connected underlying atoms be r. Then, if the expected length is $\langle l\rangle$, consistency requires that

$$\langle l\rangle = 1+r\langle l\rangle = 1/(1-r) , \tag{16}$$

when $r \ll 1$. Note that $\langle l\rangle \to \infty$ when $r \to 1$, which is exactly the condition for the percolation threshold of a tree.[25] Applying this to the Ge component we have $r \approx 2x$, whence

$$\langle l\rangle_{Ge} \approx 1/(1-2x) \tag{17}$$

with the size becoming infinite at $x=0.5$, instead of the value $x=0.56$ that was obtained form the MC growth simulations.

We now consider $\langle l\rangle$ for the phase GaAs component. If we start with a Ga atom on a {100}Ga plane we expect it to be connected to $r_{1,Ga}$ As atoms on the preceding {100}As plane, where neglecting in-plane correlations

$$r_{1,Ga}=2s_1 . \tag{18}$$

with

$$s_1=p_1/(1-p_2) . \tag{19}$$

For an As atom on a {100}As plane we will have at least one underlying Ga atom and the probable number of underlying Ga atoms is

$$r_{1,As} \approx 1+s_1 . \tag{20}$$

Consistency requires that the length starting from an As atom be

$$\langle l\rangle_{As} = 2+r_{1,Ga}r_{1,As}\langle l\rangle_{As} = 2/[1-2s_1(1+s_1)] \tag{21}$$

when $r_{1,Ga}r_{1,As}$ is small. Also, under the same condition, we must have that the length starting from a Ga atom is

$$\langle l\rangle_{Ga}=1+2s_1\langle l\rangle_{As} . \tag{22}$$

Averaging the results in Eqs. (21) and (22) we get for clusters with the phase orientation

$$\langle l\rangle_{phase}=0.5+(1+2s_1)/(1-2s_1-2s_1^2) . \tag{23}$$

Similarly for clusters with the antiphase orientation

$$\langle l\rangle_{antiphase}=0.5+(1+2s_2)/(1-2s_2-2s_2^2) , \tag{24}$$

where

$$s_2=p_2/(1-p_1) . \tag{25}$$

From Eqs. (23) and (24) we see that the clusters of either kind will become infinite when, for $s=s_1$ or s_2,

$$s>s_c=(-1+3^{1/2})/2 = 0.366 . \tag{26}$$

The resulting composition dependences of $1/\langle l\rangle$ are shown as dotted lines in Fig. 2. In the region $P_{Ge}<\frac{1}{4}$ where p_1 and p_2 are given by Eqs. (4) and (5) the phase component has $s_1>s_c$ and its domains are infinite. In contrast, the antiphase component has $s_2>s_c$ with infinite domains only when $x>0.302$ and this situation persists past $x=x_c=0.333$. In the region where $p_{Ge}>\frac{1}{4}$, both the phase and antiphase components have infinite domains until we reach $x=0.464$ when $s_1=s_2=s_c$. Thus the analytic approximation reproduces a major feature of the MC simulation, that is the coexistence of infinite phase and antiphase domains of GaAs over a range of compositions. The calculated range $0.30<x<0.46$ is in reasonable agreement with the range $0.31<x<0.42$ that was obtained from the MC experiments.

A curious feature of the analytic results is that the coexistence of infinite phase and antiphase domains extends to a region where $x<x_c$. In this range,

$0.30 < x < 0.33$, the antiphase component has an infinite domain, but is present in smaller quantity than the phase component. A similar result is suggested by the MC results where the order parameter (Fig. 3) appears to vanish at a slightly larger Ge content, $x \approx 0.34$, than $1/\langle l \rangle$ for the antiphase component at $x \approx 0.31$ (Fig. 2). It is worth noting that such behavior would not be inconsistent with physical possibility. (To return to our analogy of the interpenetrating infinite networks of the pores and the body of a sponge. There is no requirement that the pores and the material have equal volumes.)

The calculated domain depth for the Ge component is also in reasonable agreement with the MC results, with $1/\langle l \rangle \rightarrow 0$ when $x = 0.5$, instead of the MC value of $x = 0.56$. Overall we note that the composition dependences of the domain sizes give precisely the same sequence of four regions that was obtained from the MC simulation and that the boundaries of these regions occur at about the same Ge contents as in that calculation. A comparison between the results of the two approaches is given in Fig. 10.

Finally we consider analytic approximations to the NN statistics. We prohibit Ga—Ga or As—As bonds and require cation-anion symmetry, i.e., the number of As neighbors of a Ge, $N_{\mathrm{Ge,As}}$, equals the number of Ga neighbors of Ge, $N_{\mathrm{Ge,Ga}}$. The NN statistics must satisfy the general compatibility relation

$$c_i N_{i,j} = c_j N_{j,i} \ , \tag{27}$$

and the sum rule

$$\sum_j N_{i,j} = z \ , \tag{28}$$

where c_i is the concentration of the ith species (Ga, Ge, or As), $N_{i,j}$ is the number of j atoms around an i atom, and z is the total number of nearest neighbors ($z = 4$).

Since the Ga concentration equals the As concentration, the compatibility relation Eq. (27) implies that $N_{\mathrm{Ga,As}} = N_{\mathrm{As,Ga}}$. Likewise, Eq. (27) implies from the previously stated cation-anion symmetry that $N_{\mathrm{As,Ge}} = N_{\mathrm{Ga,Ge}}$. Imposing the prohibition on wrong bonds and using the sum rule in Eq. (28), we find for a Ga site

$$N_{\mathrm{Ga,As}} + N_{\mathrm{Ga,Ge}} = 4 \ . \tag{29}$$

Because of cation-anion symmetry, no new information is obtained by considering an As site. The sum rule applied to a Ge site gives

$$N_{\mathrm{Ge,Ga}} + N_{\mathrm{Ge,As}} + N_{\mathrm{Ge,Ge}} = 4 \ . \tag{30}$$

Using cation-anion symmetry and Eq. (27), we can rewrite Eq. (30) as

$$(1-x) N_{\mathrm{Ga,Ge}} + x N_{\mathrm{Ge,Ge}} = 4x \ . \tag{31}$$

Thus we have two equations [Eqs. (29) and (31)] in three unknowns.

At this point, we make an approximation that reflects the requirement that a Ga atom must always have at least one As neighbor (the pairing restriction). We say that the probability to find a Ge atom in any of the four sites around a Ge site is equal to the probability of finding a Ge atom in the three unpreempted sites around a Ga atom. Hence,

$$3N_{\mathrm{Ge,Ge}} = 4N_{\mathrm{Ga,Ge}} \ . \tag{32}$$

The three equations (29), (31), and (32) can now be solved to give

$$N_{\mathrm{Ga,Ge}} = 12x/(x+3) \ , \tag{33}$$

$$N_{\mathrm{Ge,Ge}} = 16x/(x+3) \ , \tag{34}$$

and

$$N_{\mathrm{Ga,As}} = 4(3-2x)/(x+3) \ . \tag{35}$$

The other quantity of interest is

$$N_{\mathrm{Ge,As}} = 6(1-x)/(x+3) \ . \tag{36}$$

The agreement of Eqs. (35) and (36) with the MC results in Figs. 4 and 5 is good.

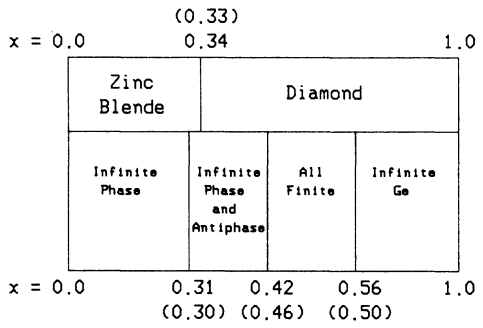

FIG. 10. Positions of the boundaries of the various alloy regions. The values of x are from the MC simulations with the approximate analytic results shown in parentheses for comparison.

V. CALCULATIONS OF THE ENERGY GAPS

In this section, we calculate the energy gap as a function of Ge concentration x for the steady-state structure obtained from the model in Sec. II. The energy bands of the pure materials can be described by a tight-binding approximation. Vogl *et al.*[26] fitted the bands with a basis set consisting of an s function, three p functions, and another, higher-energy s function (denoted sp^3s^*). In the original work, the interactions were restricted to on-site and nearest neighbors. Newman and Dow[7] have added some second nearest-neighbor interactions. This fitting determines some, but not all of the parameters needed for a tight-binding description of the alloy. New parameters such as Ga—Ge interactions are required. Fortunately those parameters that are known do not vary extensively from Ge to GaAs, so averaging to determine unknown parameters is sensible. We follow the procedure given by Newman and Dow. We have chosen the band offset to be 1 eV (Ge valence-band top higher than GaAs) to avoid having an isolated Ge atom in GaAs be a deep trap. Although this is larger than experimental values (0.3—0.5

eV),[27] the effect on the energy gap appears to be negligible for all but the smallest x values.

The energy gap is determined by calculations on a cluster of the alloy (typically of 2000 atoms). We use the Haydock recursion method[28] to calculate approximate spectral weight functions $A(k,E)$ for the cluster. Specifically, we are interested in the Γ_1 (bottom of conduction band) and the Γ_{15} (top of valence band) functions:

$$A(k=0,E)=\sum(\psi\,|\,\psi_1)^2\delta(E-E_i)\ , \tag{37}$$

where ψ is Γ_1 or Γ_{15} and ψ_i and E_i are eigenvectors and eigenvalues for the cluster. The direct gap at $k=0$ appears to be the optical gap over most of the concentration range, so we calculate only this gap. Each spectral weight function has a well-defined peak as shown in Fig. 11. For the pure materials ($x=0$ or 1), these peaks become delta functions at the band-edge energies. In the alloys, the peaks represent the complex band structure and they broaden and shift. We identify the difference between the energies of the maxima as the energy gap. Details of the numerical procedures have been published previously[29,10] and will not be repeated here. Extensive comparison with exact results and with other approximate methods (such as the coherent-potential approximate) have demonstrated that the recursion method gives accurate results for the alloy problem.[10]

In previous publications,[9,10] we emphasized the effects of SRO on the energy gap. For example, for a cluster (which has no SRO) constructed with probabilities per site of $p(Ga)=p(As)=0.25$ and $p(Ge)=0.5$, the peaks in the spectral weight functions for Γ_1 and Γ_{15} overlap, implying that the energy gap vanishes. This is an instance when one must take into account the fluctuations in the alloy potential. In the VCA, where the alloy is replaced by a crystal (diamond structure) of average atoms ($\frac{1}{4}Ga+\frac{1}{4}As+\frac{1}{2}Ge$), the calculated gap is 0.7 eV. We concluded that the VCA is not accurate enough to give reliable estimates of the small gap of this material. The primary trouble appears to be with As—As bonds in the cluster with no SRO. The sp^3s^* tight-binding approximation correctly puts the antisite (As on a Ga site in GaAs) level 0.6 eV above the valence band.[30] In the alloy with no SRO (as given by the ND model), As—As bonds introduce enough states into the region where the VCA predicts a gap that this gap vanishes. Ga—Ga bonds are not as important. The growth model forbids wrong bonds, so we expect the gap for this model to be nonzero.

A comparison of the measured optical gap of Barnett *et al.*[3] (with the data modified by Newman *et al.*[7]) with the results of the growth model (evaluated using the sp^3s^*

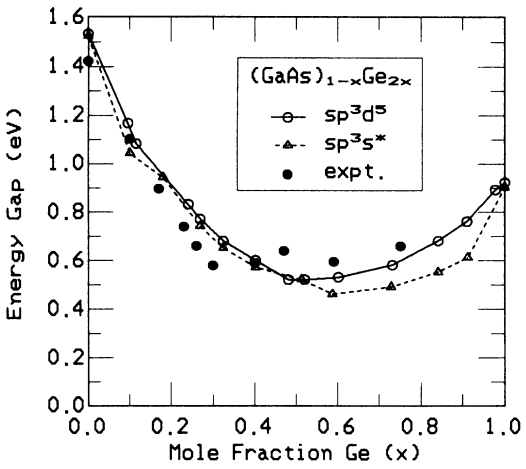

FIG. 12. Energy gap of $(GaAs)_{1-x}Ge_{2x}$. The dotted line and triangles show the recursion calculation from the sp^3s^* model. The solid line and open circles show the results of the more accurate sp^3d^5 calculation. The solid circles are experimental values from Barnett *et al.* (Ref. 3).

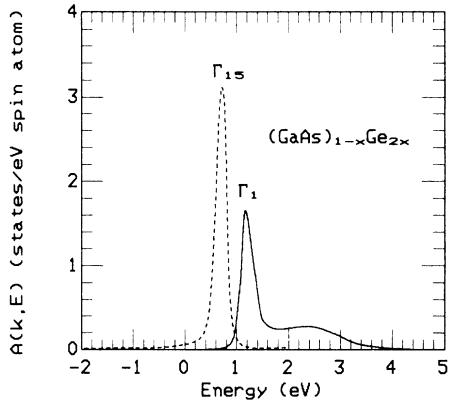

FIG. 11. Spectral weight functions for $x=0.52$ calculated with the sp^3s^* model and the recursion method. Γ_1 is the bottom of the conduction band and Γ_{15} is the top of the valence band.

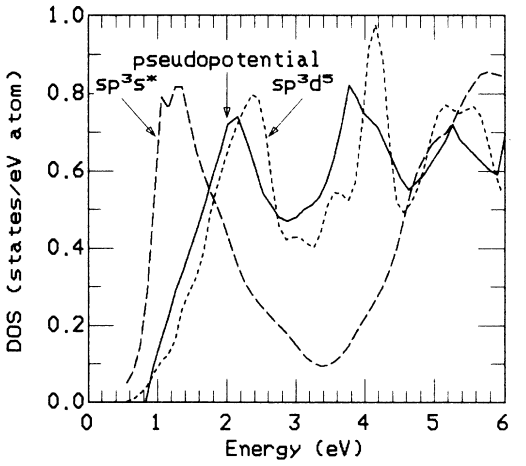

FIG. 13. The density of states (DOS) for Ge in the conduction-band region. The pseudopotential curve is from Ref. 32. The sp^3s^* and sp^3d^5 curves are obtained using the recursion method.

tight-binding approximation) is shown in Fig. 12. Both show a substantial bowing of the gap as a function of x (not a simple linear variation between end points). Each has a rapid drop in the region $x < 0.3$. For Ge-rich alloys the calculated gap is somewhat smaller than experiment, although the difference of less than 0.2 eV is comparable to the combined experimental and numerical errors. To the extent that the discrepancy is real it probably arises from inadequacies of the sp^3s^* model. Here the conduction bands are too flat, a defect common to tight-binding models, and this overemphasizes the effects of disorder. In this case, the effect is to reduce the gap.

The curve of energy gap versus x calculated for the growth model differs by less than 0.1 eV from that of our earlier percolation model.[9] Although the two models give rise to different LRO's and substantially different values of x_c (as discussed in Sec. III), their gaps are almost identical. This comes about because the two models have the same SRO, which is the dominant effect. However, if the alloy potential contained a long-range part (e.g., a Coulomb potential), the LRO of the structure would be more important. Also, the finite size of the clusters used in the calculation makes the curve smooth near the critical composition.

To eliminate the problem of flat conduction bands that the sp^3s^* tight-binding model gives, the more realistic model of Ivey and Mieher[31] has been adapted to the present problem. The Ge and GaAs pseudopotential bands of Chelikowsky and Cohen[32,33] have been fitted to the Ivey-Mieher model, which is a Koster-Slater model consisting of s, p, and d functions with first and second nearest-neighbor interactions. Here we denote this model as sp^3d^5. The two-center integrals are given in Table I. Details of the calculations will be published elsewhere.[34] Note that both models pertain to 4 K, but the experimental data were taken at room temperature where the direct gap is smaller by about 0.1 eV in Ge and GaAs.

The calculated densities of states (DOS) for Ge using the sp^3s^* and the sp^3d^5 models are compared to the pseudopotential results[32] in Fig. 13. The DOS for the sp^3d^5 more accurately reproduces the pseudopotential calculation (which we regard as the actual DOS of Ge). Since the sp^3s^* conduction bands are too flat, the first peak in the DOS is too sharp and at a lower energy than in the pseudopotential DOS. (The sp^3s^* DOS is actually much sharper than shown since our calculation was done with only 48 recursions. See Fig. 8 of the first paper of Ref. 7. We used 201 recursions for the sp^3d^5 model, so it is more accurate.) The position and sharpness of the first peak are significant because they indicate how flat the bands are

TABLE I. Two-center integrals in the sp^3d^5 model. Notation follows Ivey and Mieher (Ref. 31) with all values in eV. Separate values of the NN interactions for GaAs are listed when different [e.g., $(sp\sigma)_1$ for Ga—As and As—Ga pairs]. The second NN interactions (Ga—Ga and As—As) were constrained to be equal.

Ga	As	Ga—As	As—Ga	Ga—Ga,As—As
For GaAs				
$(ss\sigma)_0=2.620$	-6.869	$(ss\sigma)_1=-1.257$		$(ss\sigma)_2=-0.272$
$(pp\sigma)_0=6.703$	3.237	$(sp\sigma)_1=2.425$	1.528	$(sp\sigma)_2=0.324$
$(dd\sigma)_0=19.689$	19.689	$(pp\sigma)_1=4.051$		$(pp\sigma)_2=0.431$
		$(pp\pi)_1=-1.301$		$(pp\pi)_2=-0.136$
		$(pd\sigma)_1=-4.572$	-3.517	$(pd\sigma)_2=-0.125$
		$(pd\pi)_1=1.799$	0.915	$(pd\pi)_2=0.235$
		$(dd\sigma)_1=-5.140$		$(dd\sigma)_2=-0.046$
		$(dd\pi)_1=5.564$		$(dd\pi)_2=0.016$
		$(dd\delta)_1=-1.694$		$(dd\delta)_2=0.243$
		$(sd\sigma)_1=-5.470$	-4.020	$(sd\sigma)_2=-0.552$
For Ge				
$(ss\sigma)_0=-1.926$		$(ss\sigma)_1=-1.709$		$(ss\sigma)_2=-0.333$
$(pp\sigma)_0=4.399$		$(sp\sigma)_1=2.024$		$(sp\sigma)_2=0.357$
$(dd\sigma)_0=18.891$		$(pp\sigma)_1=3.814$		$(pp\sigma)_2=0.515$
		$(pp\pi)_1=-1.471$		$(pp\pi)_2=-0.217$
		$(pd\sigma)_1=-4.381$		$(pd\sigma)_2=-0.128$
		$(pd\pi)_1=1.230$		$(pd\pi)_2=0.288$
		$(dd\sigma)_1=-4.885$		$(dd\sigma)_2=-0.073$
		$(dd\pi)_1=5.747$		$(dd\pi)_2=0.106$
		$(dd\delta)_1=-1.741$		$(dd\delta)_2=0.441$
		$(sd\sigma)_1=-5.204$		$(sd\sigma)_2=-0.419$

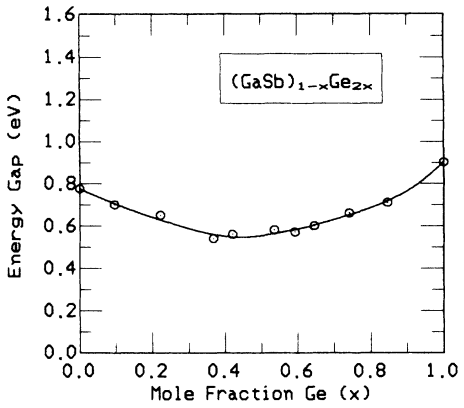

FIG. 14. Direct energy gap of $(GaSb)_{1-x}Ge_{2x}$ from the recursion calculation using the sp^3s^* model.

and, consequently, how strongly disorder scattering will affect the energy levels.[35] A related consequence is that the calculated As-antisite energy is 1.3 eV for the sp^3d^5 model, compared to the more accurate value of 0.6 eV for the sp^3s^* model. This implies that the sp^3s^* model is more reliable for calculating the effects of As—As bonds.

The sp^3d^5 values of the direct energy gap for the growth model are compared with the earlier calculations and the experimental results in Fig. 12. The Ge valence-band offset is taken to be 0.33 eV (i.e., Γ_{15} is at 0 for GaAs and 0.33 eV for Ge). We note that the sp^3s^* and the sp^3d^5 models give nearly identical results for $x<0.5$. At larger Ge concentrations the sp^3d^5 model gives larger values and agrees with experiment better. The indirect gap $(L_1-\Gamma_{15})$ is smaller than the direct gap for $x>0.9$ (approximately). The uncertainty in the calculated values of the gap is roughly 0.1 eV near the critical composition ($x_c=0.3$), but less for other concentrations. The calculated curves (for both models) do not show the sharp break at x_c that was inferred by ND, possibly for the reasons discussed above. (The break is less obvious in the original data of Barnett *et al.*[3])

Finally, in Fig. 14 we show comparable calculations for the energy gap of the alloy $(GaSb)_{1-x}Ge_{2x}$. These are predictions because there are, as yet, no published experimental data. The calculations were done with the sp^3s^* model using the parameters of Vogl *et al.*[26] No offset of the bands was included and no corrections for possible changes in bond length were made for the data displayed. For $x=0.5$, however, the calculation was repeated with an offset of 0.21 eV (Ref. 27) and scaling of the off-diagonal matrix elements by the reciprocal of the average bond length squared. The gap was found to decrease by only 0.02 eV. The EXAFS data[18] show that the bond lengths do not change as much as the average implies, so the correction is even smaller.

VI. DISCUSSION AND CONCLUSIONS

In this paper we have presented a model for the structure of the alloys $(GaAs)_{1-x}Ge_{2x}$ and $(GaSb)_{1-x}Ge_{2x}$. This is based upon the assumption that both the long- and the short-range orders arise from a combination of the statistics of arrival of the constituent atoms at the growing {100} surface with the need to avoid wrong neighbors (Ga—Ga and As—As or Sb—Sb). The model takes into account the large excess of As that is usually present during epitaxial growth of III-V compounds and their alloys from a gas phase.

The model has been implemented by Monte Carlo simulation of growth and by analytic approximations. The results of both approaches are similar and are also little affected by significant variations in the details of the growth process. We obtain excellent agreement with the measured energy gap of $(GaAs)_{1-x}Ge_{2x}$ and with the ordering and NN environments of $(GaSb)_{1-x}Ge_{2x}$ as measured by x rays, EXAFS, and Raman spectra.

ACKNOWLEDGMENTS

We thank Dr.J. R. Chelikowsky for supplying eigenvalues from his pseudopotential calculation, Dr. H. P.Hjalmarson for parameters and eigenvalues from his tight-binding model, and B. Kramer for sending order-parameter data. We are also indebted to Professor M. V. Klein, Professor J. E. Greene, and T. McGlinn for useful discussions.

[1]K. C. Cadien, A. H. Eltoukhy, and J. E. Greene, Appl. Phys. Lett. **38**, 773 (1981).

[2]S. I. Shah, K. C. Cadien, and J. E. Greene, J. Electron. Mater. **11**, 53 (1982).

[3]S. A. Barnett, M. A. Ray, A. Lastras, B. Kramer, J. E. Greene, P. M. Raccah, and L. L. Abels, Electron. Lett. **18**, 891 (1982).

[4]J. E. Greene, S. A. Barnett, K. C. Cadien, and M. A. Ray, J. Crystal Growth, **56**, 389 (1982).

[5]Zh. I. Alferov, M. Z. Zhingarev, S. G. Konnikov, I. I. Mokan, V. P. Ulin, V. E. Umanskii, and B. S. Yavich, Fiz. Tekh. Poluprovodn. **16**, 831 (1982) [Sov. Phys.—Semicond. **16**, 532 (1982)].

[6]I. Banerjee, D. W. Chung, and H. Kroemer, Appl. Phys. Lett. **46**, 494 (1985).

[7]K. E. Newman and J. D. Dow, Phys. Rev. B **27**, 7495 (1983); K. E. Newman, A. Lastras-Martinez, B. Kramer, S. A. Barnett, M. A. Ray, J. D. Dow, J. E. Greene, and P. M. Raccah, Phys. Rev. Lett. **50**, 1466 (1983).

[8]D. W. Jenkins, K. E. Newman, and J. D. Dow, Phys. Rev. B **32**, 4034 (1985).

[9]H. Holloway and L. C. Davis, Phys. Rev. Lett. **53**, 830 (1984); **53**, 1510 (E) (1984).

[10]L. C. Davis, Mater. Sci. Forum **4**, 197 (1985).

[11]The authors of Ref. 8 argued that our criticism of the VCA approach (Ref. 9) is refuted by the later observation that $(GaSb)_{1-x}Ge_{2x}$ has $x_c=0.3$ (Ref. 13), rather than the much

larger $x_c = 0.75$ predicted by the percolation model. The argument is a nonsequitur, because the applicability of the VCA to this alloy and the position of its order-disorder transition are unrelated issues. We showed that the VCA gave the wrong energy gap for $(GaAs)_{1-x}Ge_{2x}$, even in the case when it was applied to the ND model (with $x_c = 0.3$).

[12]B. Koiller, M. A. Davidovich, and R. Osorio, Solid State Commun. **55**, 861 (1985).

[13]S. I. Shah, B. Kramer, S. A. Barnett, and J. E. Greene, J. Appl. Phys. **59**, 1482 (1986).

[14]T. N. Krabach, N. Wada, M. V. Klein, K. C. Cadien, and J. E. Greene, Solid State Commun. **45**, 895 (1983).

[15]R. Beserman, J. E. Greene, M. V. Klein, T. N. Krabach, T. C. McGlinn, L. T. Romano, and S. I. Shah, in *Proceedings of the 17th International Conference on the Physics of Semiconductors,* edited by J. D. Chadi and W. A. Harrison (Springer, New York, 1985), p. 961.

[16]K. E. Newman, J. D. Dow, A. Kobayashi, and R. Beserman, Solid State Commun. **56**, 553 (1985); A. Kobayashi, K. E. Newman, and J. D. Dow, Phys. Rev. B **32**, 5312 (1985).

[17]References 14 and 15 describe original Raman data. Reference 16 is an interpretation in which the authors assert that the LO-TO splitting decreases to zero as $x \rightarrow 0.3$. This claim is not consistent with the experimental data shown in Fig. 2 of Ref. 15. In fact, the authors of Ref. 15 state categorically that such a splitting cannot be detected when $x > 0.1$.

[18]E. A. Stern, F. Ellis, K. Kim, L. Romano, S. I. Shah, and J. E. Greene, Phys. Rev. Lett. **54**, 905 (1985).

[19]The authors of Ref. 15 state specifically that they failed to find evidence for Sb—Sb NN pairs, which they would have expected to detect had these been present in the concentrations that are predicted by the ND model.

[20]K. Kim and E. A. Stern, Phys. Rev. B **32**, 1019 (1985).

[21]The samples of the percolation model were obtained by putting Ge and GaAs onto successive {100} planes of a diamond lattice. This process somewhat resembles the growth simulations of KS and of the present paper. We discuss the relationship between the models later in Sec. III.

[22]H. Holloway and L. C. Davis, Phys. Rev. B (to be published). This paper deals with simulations of ⟨111⟩ growth. In particular we note that growth along the ⟨111⟩As direction no longer gives an order-disorder transition near $x_c = 0.3$. Instead some residual zinc-blende order is predicted to persist so long as any of the GaAs constituent is present (i.e., $x_c = 1$). A further prediction is that growth along ⟨111⟩Ga is metastable, with a tendency to convert spontaneously to ⟨111⟩As when $x > 0.1$.

[23]L. C. Davis, H. Holloway, and L. A. Feldkamp, in Proceedings of the 13th Midwest Solid State Physics Theory Symposium, University of Notre Dame, 1985 (unpublished).

[24]The authors of Ref. 18 fitted the number of Sb NN's of a Ga atom to a linear composition dependence, $N_{Sb} = 4(1-x)$, which they asserted corresponds to the perfect SRO of our percolation model. This is inaccurate on two counts. First, our percolation model assumed (as does the growth model) that the group III and group V atoms occur as III-V NN pairs. Thus, we cannot possibly be in agreement with a relationship that can give $N_{Sb} < 1$. Second, the asssumption that N_{Sb} is a linear function of x is unjustified and probably incorrect. Both the MC results and an analytic approximation for N_{Sb} show significant curvature, which allows respectable agreement with the data, despite the fact that the model requires that $N_{Sb} \rightarrow 1$ when $x \rightarrow 1$.

[25]M. E. Fisher and J. W. Essam, J. Math. Phys. **2**, 609 (1961).

[26]P. Vogl, H. P. Hjalmarson, and J. D. Dow, J. Phys. Chem. Solids **44**, 365 (1983); H. P. Hjalmarson, Ph.D. thesis, University of Illinois, 1979; and private communication.

[27]A. D. Katnani and G. Margaritondo, Phys. Rev. B **28**, 1944 (1983).

[28]R. Haydock, in *Solid State Physics,* edited by H. Ehrenreich, F. Seitz, and D. Turnbull (Academic, New York, 1980), Vol. 35, p. 215.

[29]L. C. Davis, Phys. Rev. B **28**, 6961 (1983).

[30]E. R. Weber, H. Ennen, U. Kaufmann, J. Windscheif, J. Schneider, and T. Wosinski, J. Appl. Phys. **53**, 6140 (1982); B. K. Meyer, J.-M. Spaeth, and M. Scheffler, Phys. Rev. Lett. **52**, 851 (1984).

[31]J. L. Ivey and R. L. Mieher, Phys. Rev. B **11**, 849 (1975). Also see S. G. Louie, Phys. Rev. B **22**, 1933 (1980). In this paper, accurate bands for Si, Ge, and trigonal Se were obtained using a basis set consisting of *s*, *p*, and *d* functions. The calculated matrix elements of the Hamiltonian were not published, and so they could not be used in the present work. As many as fifth-nearest-neighbor interactions were included in the evaluation of matrix elements. Such a large number of neighbors would be impractical to treat with the recursion method.

[32]J. R. Chelikowsky and M. L. Cohen, Phys. Rev. B **14**, 556 (1976); M. L. Cohen and J. R. Chelikowsky, in *Handbook on Semiconductors,* edited by T. S. Moss and W. Paul (North-Holland, New York, 1982), Vol. 1, p. 219.

[33]J. R. Chelikowsky (private communication).

[34]L. C. Davis (unpublished).

[35]Y. Onondera and Y. Toyozawa, J. Phys. Soc. Jpn. **24**, 341 (1968).